Journal of Radiation Research and Applied Sciences 18 (2025) 101229

Contents lists available at ScienceDirect

Journal of Radiation Research and Applied Sciences

journal homepage: www.journals.elsevier.com/journal-of-radiation-research-and-applied-sciences

Green synthesis and anticancer activity of titanium dioxide nanoparticles using the endophytic fungus *Aspergillus* sp.

Hani A. Alhadrami [a,b,c], Hossam M. Hassan [d,e], Albaraa H. Alhadrami [f], Mostafa E. Rateb [f,*], Ahmed A. Hamed [g]

[a] Faculty of Applied Medical Sciences, Department of Medical Laboratory Sciences, King Abdulaziz University, P. O. Box 80402, Jeddah, 21589, Kingdom of Saudi Arabia
[b] King Fahd Medical Research Centre, DNA Forensic Unit, King Abdulaziz University, P. O. Box 80402, Jeddah, 21589, Kingdom of Saudi Arabia
[c] King Abdulaziz University Hospital, Molecular Diagnostics Lab, P. O. Box 80402, Jeddah, 21589, Kingdom of Saudi Arabia
[d] Department of Pharmacognosy, Faculty of Pharmacy, Beni-Suef University, Beni-Suef, 62514, Egypt
[e] Department of Pharmacognosy, Faculty of Pharmacy, Nahda University, Beni-Suef, 62513, Egypt
[f] School of Computing, Engineering & Physical Sciences, University of the West of Scotland, Paisley, PA1 2BE, UK
[g] Microbial Chemistry Department, National Research Centre, 33 El-Buhouth Street, Dokki, Giza, 12622, Egypt

ARTICLE INFO

Keywords:
Titanium dioxide nanoparticles
Aspergillus
Anticancer
MMP-3
Molecular dynamic simulations
MCF7

ABSTRACT

Titanium dioxide nanoparticles (TiO_2 NPs) have attracted significant attention for their unique physicochemical features and various applications. This study demonstrated the biosynthesis of TiO_2 NPs using *Aspergillus* fungal extract that served as a green and eco-friendly reducing and stabilizing agent. The biosynthesized nanoparticles were analyzed using SEM and TEM to determine their morphology, size, and distribution, FTIR to determine functional groups, and Zeta potential to assess their surface charge and stability. An extensive review of the Protein Data Bank (PDB) and literature indicated that TiO_2 could target various cancer-relevant matrix metalloproteinases. In vitro screening indicated promising anticancer effects against the MCF7 breast cancer cell line. To investigate the possible mode of action of TiO_2 NPs as an anticancer agent, human matrix metalloproteinase-3 was highlighted as a protein inhibited by metallic ions like $PtCl_2$. Therefore, we investigated whether TiO_2 could similarly interact with the active site of MMP-3. We hypothesized that TiO_2 could interact with the MMP-3 active site and replace $PtCl_2$ with modelled TiO_2 in its co-crystallized binding site. A 100 ns-long MDS, binding free energy (ΔGBinding) of $PtCl_2$ and TiO_2 within MMP-3 binding site indicated that TiO_2's enhanced binding affinity and stability, as evidenced by a ΔGBinding of −7.23 kcal/mol and average RMSD of 0.89 Å, compared to $PtCl_2$'s lower affinity. In conclusion, endophytic fungi can be used efficiently in the biosynthesis of nanoparticles. Our study indicated TiO_2 NPs have a potential anticancer effect, suggesting TiO_2 binds to MMP3, potentially offering comparable inhibitory effects on the enzyme's activity.

1. Introduction

Recently, the use of nanoparticles has attracted researchers' attention due to their unique characteristics and wide range of applications. The selection of the experimental technique for synthesizing nanomaterials is a key step in controlling the formation of nanoparticles with appropriate chemical compositions, sizes, and high monodispersed shapes, which is considered a vital factor of nanotechnology (Li et al., 2019). Researchers have been very interested in materials with nanoscale dimensions because of their exponential potential in nearly every field of endeavor. Titanium dioxide nanoparticles (TiO_2 NPs) are extensively utilized in diverse industries dealing with plastics, textiles, food and cosmetic products, sunscreen components, ceramics, ink and paints, as well as reducing the toxicity of dyes and pharmaceutical drugs. They were also studied as photosensitizing agents in the treatment process of malignant tumors and photodynamic inactivation of resistant bacterial strains (Ziental et al., 2020). TiO_2 is a substance of great technical importance, particularly as a dielectric, with diverse applications in photovoltaics, photocatalysts, batteries, etc (Khan & Sultana, 2019). As a result, great intention has been given to the

* Corresponding author.
E-mail addresses: hanialhadrami@kau.edu.sa (H.A. Alhadrami), hossam.abdelazeem@pharm.bsu.edu.eg (H.M. Hassan), albaraa.h.alhadrami@gmail.com (A.H. Alhadrami), Mostafa.Rateb@uws.ac.uk (M.E. Rateb), ahmedshalbio@gmail.com (A.A. Hamed).

https://doi.org/10.1016/j.jrras.2024.101229
Received 29 August 2024; Received in revised form 9 November 2024; Accepted 27 November 2024
Available online 30 November 2024

biosynthesis of titanium dioxide nanostructures. Due to its remarkable UV-filtering properties, notable catalytic, and significant photochemical activities, TiO_2 NPs have drawn a lot of attention (Punitha et al., 2020; Ramya et al., 2022; Vembu et al., 2022; Nilavukkarasi et al., 2022).

For any technology to be accepted, minimum time, miniaturization, and non-hazardous procedures are essential. Although nanoparticles have been successfully synthesized employing different physical and chemical methods, their noticeable drawbacks, especially the use of toxic chemicals and the high energy required, have encouraged researchers to focus more on the biosynthesis of nanoparticles, a more environmentally friendly way to synthesize inorganic materials (Shyamalagowri et al., 2022). Biological synthesis is an alternative method for producing these nanoparticles. The environmentally safe and cost-effective method of producing nanoparticles using fungal extract is currently receiving a lot of interest because of its scalability, pure chemical surfaces, and, most notably, its use in biology and medicine (Dzulkharnien & Rohani, 2022).

Fungi are promising biological objects for the green synthesis of nanoparticles. Biogenic synthesis of nanoparticles in fungal cultures is an easy and environmentally friendly method. Fungi are known to produce diverse biologically active compounds and have a robust enzymatic system that enables them to biosynthesize nanoparticles of chemical elements. Using different synthesis conditions, the same fungal culture could produce nanoparticles with various shapes and sizes, offering different biological activities (Loshchinina et al., 2022). The biosynthesis of TiO_2 NPs has broad interest among researchers due to its reproducibility, cost-effectiveness, and eco-friendliness (Waghmode et al., 2019).

In the present study, we aimed to utilize the plant-derived endophyte *Aspergillus* AT22 fungal extracts to direct the biosynthesis of TiO_2 NPs. After their characterization, TiO_2 NPs were evaluated for their antibacterial and anticancer activities in vitro. Additionally, the mechanism of their promising anticancer effect of TiO_2 NPs is proposed using in-depth in silico analysis.

2. Materials and methods

2.1. Chemical and reagent

Titanium Tetrachloride ($TiCl_4$) was obtained from Sigma-Aldrich. All media and solvents were purchased from Merck and Fisher.

2.2. Sample collection

Sample collection was carried out in May 2018 from Wadi El Natroun, Egypt. The collected plant samples were coded, photographed, and Kept at 4 °C till further analysis.

2.3. Isolation of endophytic fungi from plant samples

The isolation of endophytic fungi from the collected plant (*Alhagi graecorum*) was carried out using surface sterilization methods using 70% ethanol. After sterilization, the plant leaves were cut and placed on potato dextrose agar (PDA) medium supplemented with 100 mg/L ampicillin and 50 mg/L streptomycin. Fungal colonies were allowed to grow on the plates by incubating them at 25 °C.

2.4. Genetic identification of fungal strains

The fungal strain was sub-cultured for 3 days at 25 °C in potato dextrose broth media. Pure distinct colonies were dispersed in a sterile saline solution (0.5 mL). The suspension was then centrifuged at 10,000 rpm for 10 min at room temperature. The DNA was extracted using a DNeasy Blood & Tissue Kit per the manufacturer's protocol. ITS2, GCTGCGTTCTTCATCGATGC, and ITS3, GCATCGATGAAGAACGCAGC, were used as primers. The PCR reaction was conducted as follows: 35 cycles of 30s at 94 °C, then 30s at 55 °C, 90s at 72 °C, with a final step of 5 min at 72 °C. The PCR products were then cleaned of unincorporated PCR primers and dNTPs using a Montage PCR Clean-up kit (Millipore). Two primers were used to sequence the purified PCR product: ITS1, TCCGTAGGTGAACCTGCGG, and ITS4, TCCTCCGCTTATTGATATGC. An automated DNA-sequencing device from Applied Biosystems, model 3730-XL, was used to resolve the sequencing results.

2.5. Fungal filtrate preparation

The fungus was grown in potato dextrose (PD) medium by dissolving 24 g of potato dextrose medium in 1 L dH_2O and autoclaved for 15 min at 121 °C. After autoclaving, the endophytic fungi were inoculated into the PD broth by transferring a small piece of fungal mycelium from the PDA plate into the broth using a sterile loop. The flasks were then incubated at 25 °C for 7 days with constant shaking. After 7 days of cultivation, the fungal mycelia were removed from the broth by filtration through filter paper. Then, the filtrate was centrifuged at 10,000 rpm for 10 min. The resulting supernatant was used for further analysis.

2.6. The biosynthesis of TiO_2 NPs

The biosynthesis of TiO_2 NPs experiment was carried out by combining 25 mL of fungal supernatant with 25 mL of 1 mM TiO_2 solution (prepared in deionized water). The mixture was then placed in a shaker incubator at 200 rpm in a dark environment at 37 °C for 24 h. Two control groups were simultaneously established under the same conditions: a positive control where the fungus supernatant was incubated with deionized water, and a negative control containing only the TiO_2 solution. After preparation, the precipitate was washed several times using deionized water and centrifuged at 10,000 rpm to remove unreacted substances and impurities.

2.7. Characterization of TiO_2 NPs

2.7.1. UV-spectroscopy

The UV spectral analysis was carried out between 200 and 800 nm by a UV spectrophotometer (Shimadzu Corporation, Japan) for UV–visible spectral analysis.

2.7.2. FTIR

Fourier transform infrared (FT-IR) analysis was performed using an FT-IR 6100 spectrometer (Jasco, Japan) in the 4000–400 cm^{-1} range to describe the functional groups present in TiO2 NPs.

2.7.3. Zeta potential measurements

The stability and charges of the synthesized nanoparticles were assessed using a zeta sizer nano-z's laser diffractometer (Malvern, UK) to conduct zeta potential measurements.

2.7.4. X-ray diffraction (XRD)

The prepared solid materials were subjected to X-ray diffraction (XRD) analysis using a Bruker D8 Advance Diffractometer (Bruker AXS, Germany) with Cu Ka radiation (k = 1.54) to obtain the XRD pattern of TiO_2 NPs within a 2θ range of 10–90°.

2.7.5. Transmission electron microscopy

The biosynthesized TiO_2 NPs shape and size were visualized using a JEOL-JEM-1011 (Japan). A droplet of nanoparticles was put on a carbon-covered copper grid and used for analysis.

2.8. Antibacterial assay

Antimicrobial activity of the biosynthesized TiO_2 NPs was carried out according to Elkhouly et al. (2021). Gram + ve *S. aureus* ATCC25923 and Gram -ve *Escherichia coli* ATCC8739 were used as test microbes in a

96-well Polystyrene plate. Briefly, 10 µL of the test material (final concentration of 250 µg/mL) was mixed with 150 µL of LB broth. Each well was then inoculated with 10 µL of log-phase bacterial culture. Then, the plates were incubated at 37 °C for 24 h. Following the incubation period, a clean zone, or clearance, in the wells indicated that the tested chemicals had a favorable antibacterial action and were inhibiting bacterial growth. After about 20 h, the samples' absorbance was measured at OD600 using a Spectrostar Nano Microplate Reader (BMG LabTech GmbH, Allmendgrun, Germany) to determine the antibacterial activity. Thanks to this measurement, the researchers quantitatively evaluated the impact of TiO_2 NPs on the bacterial and fungal cultures.

2.9. Anticancer assay

The cytotoxic effect of TiO_2 NPs generated by *Aspergillus* sp. AT22 culture supernatant and cell filtrate were evaluated against human MCF-7 and HepG-2 cancer cell lines using sulphorhodamine B assay (SRB). Human tumor cells were seeded in a 96-well tissue culture plate at 90% confluence, cultured for 24 h, and then treated with the biosynthesized TiO_2 NPs at various concentrations (0.01, 0.1, 1, 10, and 1000 µg/mL). Untreated cells were used as a control. Cells were exposed to nanoparticles for 72 h, fixed with 10% trichloroacetic acid for 1 h at 4 °C, and stained with 0.4% SRB solution for 10 min. The extra stain was removed by rinsing with a 1% solution of glacial acetic acid, after which the cells stained with SRB were dissolved using Tris-HCl. The color intensity was measured at 540 nm by a microplate reader. To calculate the IC_{50} values, the cell viability percentages at different TiO_2 NPs concentrations were analyzed using SigmaPlot 12.0 software.

2.10. In silico study

2.10.1. Modeling of TiO_2

The titanium dioxide (TiO_2) molecule was modelled using the Spartan20 software (Setty, 2020). The initial step involved the creation of a basic three-dimensional model of TiO_2 structure by adding its empirical formula into the construct function in Spartan20. The most stable molecular conformer was determined by geometry optimization using a 6-31G* basis set and the Hartree-Fock technique. Then, we have applied the Density Functional Theory (DFT) and the B3LYP functional to calculate the electronic structures of the molecules due to their accuracy and reproducibility. Then, a frequency analysis was performed to verify the optimized structure's stability and exclude imaginary frequencies that indicate the presence of transition states. The final optimized molecular structure and its electrical properties were further visualized by Spartan20's graphical capabilities.

2.10.2. Molecular dynamics simulation

NAMD 3.0 software (Phillips et al., 2005; Ribeiro et al., 2018) was used to perform the Molecular Dynamics Simulations (MDS), implementing the Charmm-36 force field. The VMD program's inbuilt QwikMD toolbox was used to prepare the protein systems (Humphrey et al., 1996). A physiological pH of 7.4 was maintained by removing any co-crystallized water molecules and adjusting the protonation status of all amino acid residues. Then, the whole protein complex was enclosed in an orthorhombic box of 20 Å in diameter, filled with TIP3P water, and supplemented with 0.15M of Na^+ and Cl^- ions. Thereafter, the systems underwent a 5 ns equilibration and energy minimization. Next, the modelled TiO_2 molecule was accurately positioned at the coordinates of the $PtCl_2$ crystallized ligand inside the protein structure. The characteristics and topologies of the TiO_2 molecule were accurately calculated using the VMD plugin Force Field Toolkit (ffTK), which allowed further improvement of the simulation. Consequently, the resulting parameters and topology files were imported into VMD to analyze the protein-ligand complexes and perform the simulation stages.

2.10.3. Binding free energy calculations

The Molecular Mechanics Poisson-Boltzmann Surface Area (MM-PBSA) incorporated into the MMPBSA.py module of AMBER18 was employed to compute the binding free energy of the docked complex (Miller III et al., 2012). A total of 100 frames were analyzed from the trajectories, and the system's net energy was calculated using the following equation:

$$\Delta G_{\text{Binding}} = \Delta G_{\text{Complex}} - \Delta G_{\text{Receptor}} - \Delta G_{\text{Inhibitor}}$$

Each of the aforementioned terms requires calculating multiple energy components, including van der Waals energy, electrostatic energy, internal energy from molecular mechanics, and polar contribution to solvation energy.

2.11. ADME prediction

The ADME predictions for TiO_2 molecule were conducted using the methods described by Swanson et al. (2024) without any modifications.

3. Results

3.1. Isolation of the fungal strain

Processing of the collected plant sample (*Alhagi graecorum,* Fig. 1a) led to the isolation of the fungal strain AT22 (Fig. 1b). Based on their physical traits, the fungal colonies were identified (Fig. 1b). The obtained strains were tagged, and stored in a culture collection at 4 °C till being used.

3.2. Genetic identification of the isolated fungal strains

The isolated fungus AT22 was identified by conducting a sequencing analysis of the 18S rRNA gene, following a preliminary investigation of the isolated fungus AT22. The DNA of the fungal sample was obtained, identified, and compared to existing sequences in the GenBank database using the BLAST tool (http://www.blast.ncbi.nlm.nih.gov/Blast, accessed on June 20, 2024). This was done to determine the similarity score and statistical significance of the matches. The isolate's 18S rRNA gene sequences were found to be identical with *Aspergillus* sp., showing 100% identity, according to the data. The strain was identified and deposited with accession number OR327425 in GenBank. The Tamura-Nei model and the Maximum Likelihood approach (Tamura et al., 2004) were used to construct the evolution history (Fig. 2). The percentage of trees that contain related taxa was displayed next to the branches. A pairwise distances matrix was generated using the Tamura-Nei model, and the topology with the highest log-likelihood value was selected as the starting tree for the heuristic search. Evolutionary research was carried out using MEGA X software (Kumar et al., 2018).

3.3. Biogenic synthesis of TiO_2 NPs

when the fungal culture reached the required growth phase, its filtrate was obtained through a sterilized filter paper. This filtrate comprised all fungal enzymes and biomolecules that could convert titanium ions into TiO_2 NPs through reduction. To achieve this, the obtained filtrate was combined with a solution containing titanium ions (titanium tetrachloride). Then, the resulting mixture was incubated at 37 °C for 24hr. The biosynthesis of TiO_2 NPs was controlled by the enzymes and biomolecules in the fungal filtrate, which acted as reducing agents that catalyzed the reduction and conversion of titanium ions into TiO_2 NPs.

3.3.1. UV–vis analysis

The green TiO_2 NPs formed by fungal extract were monitored by UV–visible spectroscopy and the color change. The formation of TiO_2

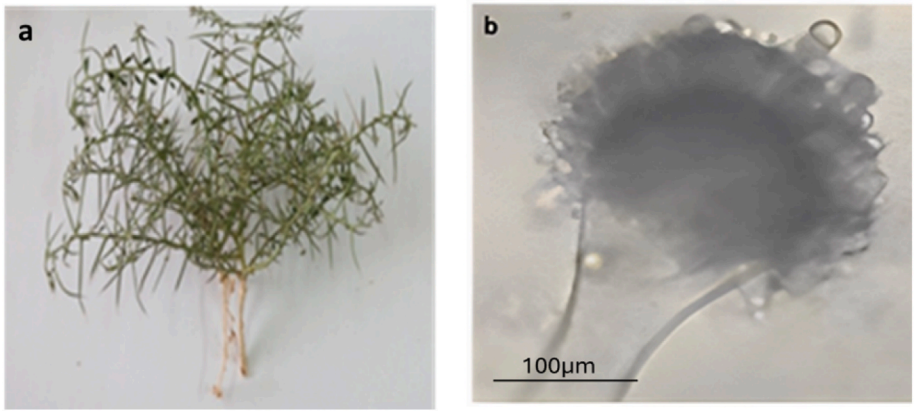

Fig. 1. a) *Alhagi graecorum* plant, b) Morphological identification of isolate AT22.

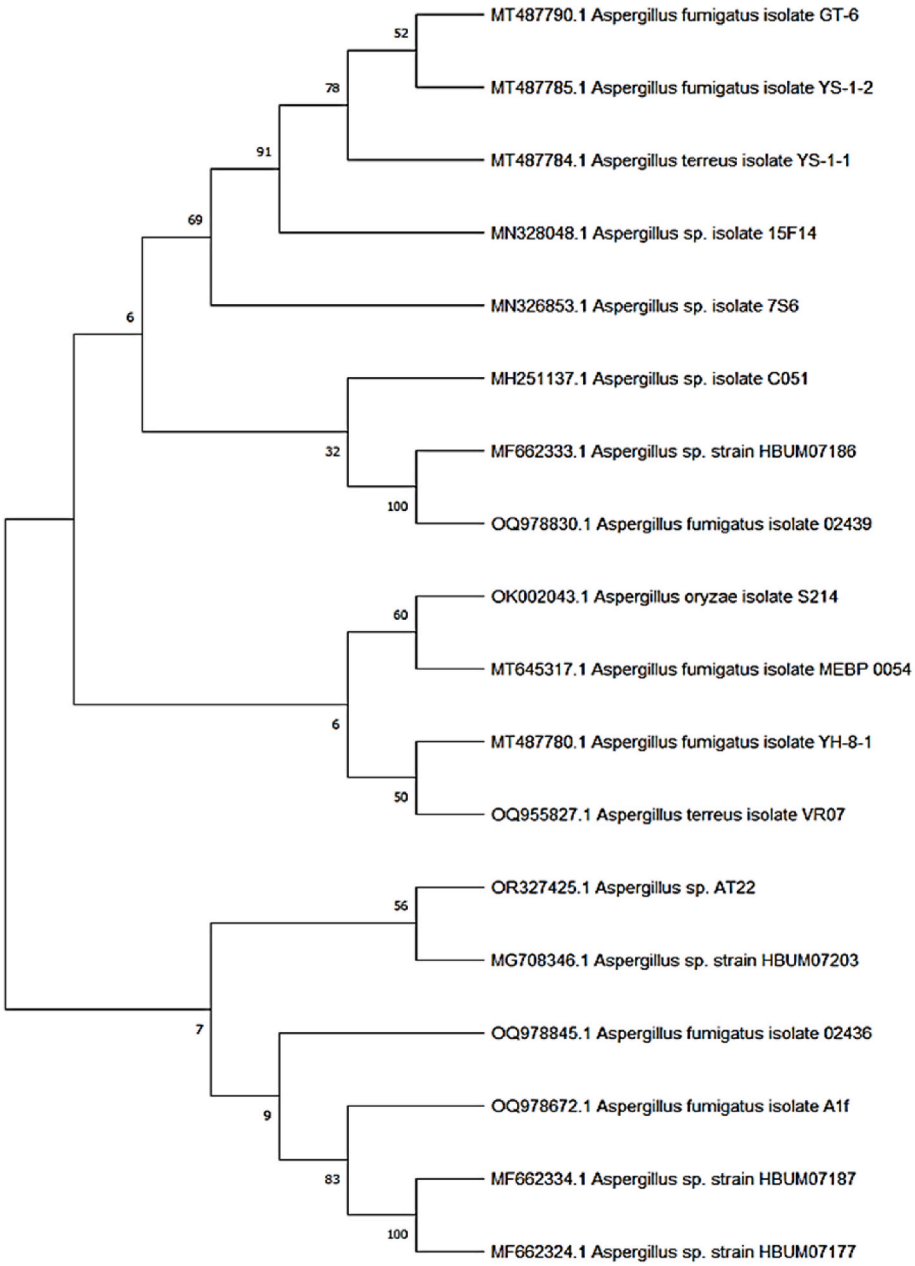

Fig. 2. Constructed phylogenetic tree of isolate AT22.

NPs from titanium tetrachloride solution started with a dramatic color change, from a brownish-red to a light white color. UV–Vis spectroscopy analysis was also used to monitor the formation of TiO_2 NPs. The appearance of a plasmon band between 330 and 380 nm, as shown in Fig. 3c, indicated the formation of TiO_2 NPs.

3.3.2. Fourier transforms infrared spectroscopy (FTIR) analysis

Fig. 4 depicted the FTIR analysis performed on the extract and the resulting titanium nanoparticles to identify the functional groups accountable for the synthesis and stability of the nanoparticles. The FTIR spectral profile of TiO_2 NPs displayed characteristic peaks at 3423, 3250, 2870, 1610, 1525, 1310, 1200, and 1070 cm^{-1}, corresponding to various functional groups. These groups, including OH, CH, C=O, C=C, C-O, C-N, and C-C, were found in the prepared NPs (Fig. 4). Specifically, the stretching vibration of the hydroxyl group (O-H) was observed at 3423 cm^{-1}, while peaks at 2870 cm^{-1} indicated the stretching vibration of alkane (C-H) bonds. Furthermore, carbonyl (C=O) stretch vibration was identified at 1610 cm^{-1}. The C-O group was detected at 1310 cm^{-1}, and the band at 1200 cm^{-1} corresponded to C-N stretching. Furthermore, the presence of C-C bonds was confirmed at 1070 cm^{-1}. The absorption bands corresponding to C=C, C=O, C-O, C-N, OH, and CH mainly arise from the bioactive natural molecules present in the fungal extract. These functional groups played a crucial role in reducing titanium metal ions, leading to the synthesis of TiO_2 NPs, and contributed significantly to the stability of the prepared nanoparticles.

3.3.3. Zeta potential of synthesized TiO_2 NPs

The stability of TiO_2 NPs colloids in a neutral aqueous medium (distilled water) could be attributed to their zeta potential value of −22.03 mV. Zeta potential is a crucial parameter that reflects the surface charge of nanoparticles in a solution. When nanoparticles possess a high absolute zeta potential value (positive or negative), they repel each other, thereby hindering their agglomeration or aggregation. Stability was critical since nanoparticles' propensity to combine might significantly impact their characteristics and efficacy in various applications (Phan & Haes, 2020; Varshney, Bhadauria, & Gaur, 2019). In the case of TiO_2 NPs with a negative zeta potential value of −22.03 mV, they experience mutual electrostatic repulsion, which helped to maintain their dispersion and stability in the solution (Table 1).

3.3.4. X-ray diffraction (XRD) pattern analysis

The experimental XRD pattern closely matched the JCPDS card no. 21–1272, which corresponded to the anatase phase of TiO_2, which was consistent with the recent findings by Antić et al. (Antić et al., 2012), which confirmed the presence of anatase TiO_2 NPs. The diffraction peak at $2\theta = 25.4°$ confirmed the TiO_2 crystal structure, supporting the findings of Ba-Abbad et al. (Ba-Abbad, Kadhum, Mohamad, Takriff, &

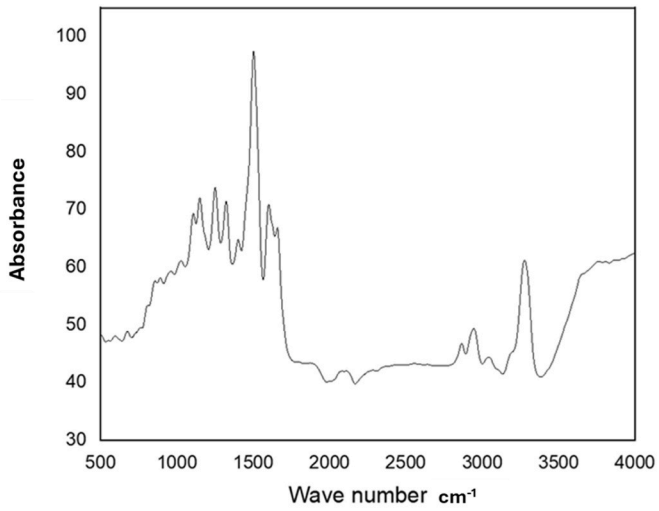

Fig. 4. FTIR for TiO_2 NPs.

Table 1
Zeta potential analysis of synthesized TiO_2 NPs.

NPs	Mean hydrodynamic diameter (nm)	ζ potential (mV)
TiO_2 NPs	152 ± 14	−22.03 ± 6.21

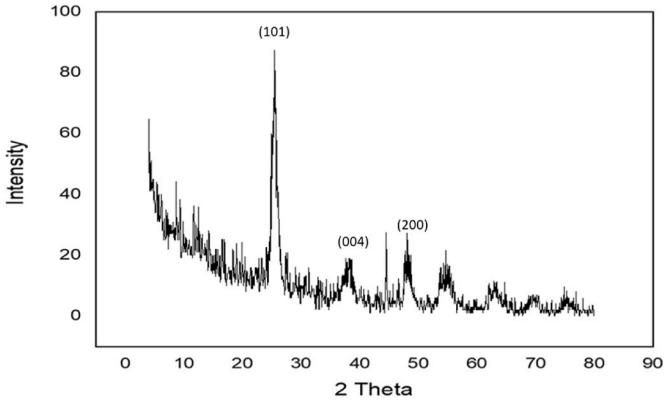

Fig. 5. The XRD diffraction pattern of the green synthesized TiO_2 NPs.

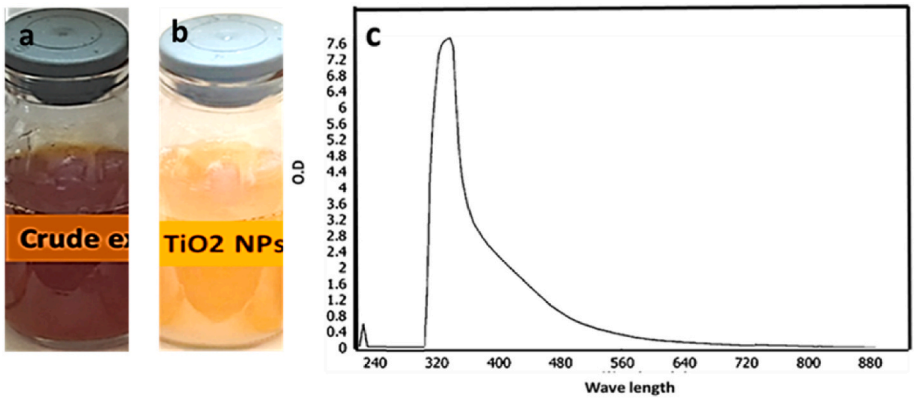

Fig. 3. (a,b) Color change due to formation of titanium dioxide nanoparticles (c) UV spectrum of biogenic TiO_2 NPs. (For interpretation of the references to color in this figure legend, the reader is referred to the Web version of this article.)

Sopian, 2019). Strong diffraction peaks at 25° and 48° confirmed the existence of TiO_2 in the crystal phase, according to Thamaphat, Limsuwan, and Ngotawornchai (2019) (see Fig. 5).

3.3.5. Transmission and scanning electron microscopy (TEM and SEM) studies

The particle size and crystallinity of TiO_2 NPs were studied (HR-TEM) and (SEM) (Fig. 6a and b). The results, shown in Fig. 6, revealed that the particles were made up of polydisperse crystals, with an average particle size ranging from 1.36 to 20 nm. Small particle aggregates inside these spherical crystals averaged 24–62 nm in size. These results were consistent with the X-ray data, demonstrating coherence between the two characterization approaches.

3.4. Biological evaluation

3.4.1. Antimicrobial activity of TiO_2 NPs

When the biosynthesized TiO_2 NPs were tested for their antibacterial effect, they displayed weak antibacterial activity against tested pathogenic bacteria (Fig. 7). This result agreed with previous reports indicated that TiO_2 NPs exhibit antibacterial activity only when exposed to UV light. This phenomenon is attributed to the photocatalytic properties of TiO_2, specifically its ability to generate ROS such as hydroxyl radicals, superoxide ions, and singlet oxygen when exposed to UV light. These ROS have strong oxidative properties, which can damage bacterial cell membranes, proteins, and DNA, leading to bacterial death (Komine et al., 2022).

3.4.2. Anticancer potentiality of TiO_2 NPs

The obtained cytotoxicity results of TiO_2 NPs toward two cell lines (MCF7 and HepG-2) cells showed significant differences in their IC_{50} values. The IC_{50} value for MCF7 cells was 11.2 ± 0.57 µg/mL, while for HepG-2 cells, it was 31.1 ± 1.44 µg/mL (Fig. 8). This result would indicate a selective cytotoxicity of TiO_2 NPs toward MCF7 breast cancer cells.

3.5. In silico study

After performing an in-depth review of the relevant literature in all scientific databases and a comprehensive analysis of cancer-related proteins listed in the Protein Data Bank (PDB), we found that titanium dioxide (TiO_2) and its nano-formulations are substances that have been shown to interact with different matrix metalloproteinases (Armand et al., 2011; Belviso et al., 2013; Nasr et al., 2018). Among the obtained results, $PtCl_2$ and other metallic ions have been demonstrated the efficient targeting and inhibiting human matrix metalloproteinase-3 (MMP-3; PDB ID: 4DPE), a protein that strongly associated with cancer progression in different human cancers (Mendes et al., 2005).

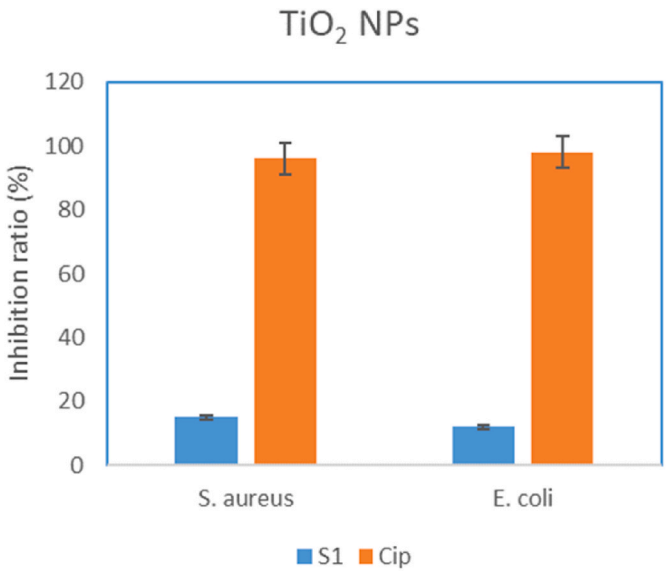

Fig. 7. Antibacterial activity of biogenic TiO_2 NPs.

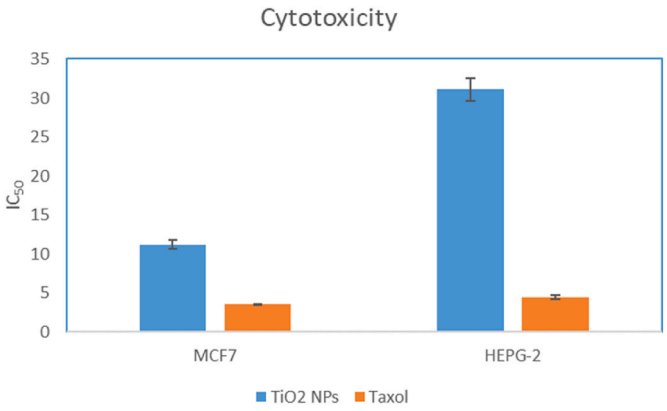

Fig. 8. Anticancer activity of biogenic TiO_2 NPs.

These findings encouraged us to investigate the possibility of TiO_2 to interact with the MMP-3 active site, likewise $PtCl_2$. Then, we substituted $PtCl_2$ for a modelled TiO_2 molecule at its co-crystallized binding location to computationally test our hypothesis. The original co-crystallized complex and this freshly formed complex were then subjected to a 100 nsMolecular Dynamics (MD) simulation. Our main objective was the evaluation of the total stability of $PtCl_2$ and TiO_2 in the MMP-3

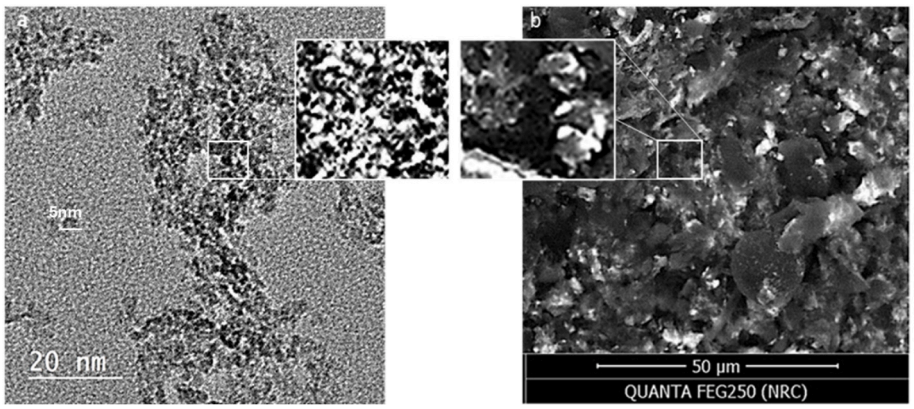

Fig. 6. TEM analysis (a) and SEM analysis (b) of synthesized TiO_2 NPs.

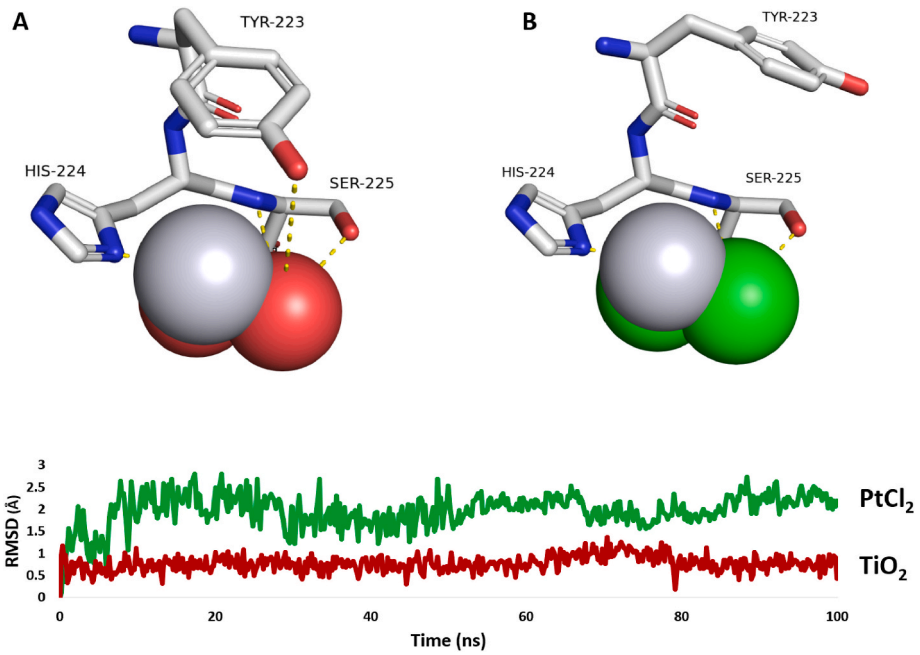

Fig. 9. Binding modes of both TiO_2 and $PtCl_2$ inside the MMP3's binding site (PDB ID: 4DPE; A and B, respectively). RMSD profiles of both TiO_2 and $PtCl_2$ inside the MMP3's binding site over the course of 100 ns-long MD simulation.

binding site and the absolute binding free energy (Δ*G*_binding) (Fig. 9).

As demonstrated in Fig. 9A, the interaction of TiO_2 within the enzyme active site exhibited consistent stability throughout the 100 ns molecular dynamics simulation (MDS). This was evidenced by a calculated binding free energy (ΔGBinding) of −7.23 kcal/mol and an average root-mean-square deviation (RMSD) of 0.89 Å. $PtCl_2$ showed reduced binding affinity and stability, with ΔGBinding of −6.26 kcal/mol and RMSD of 2.11 Å. TiO_2's enhanced binding effectiveness could result from creating an additional hydrogen bond with TYR 223. As a result of these MDS findings, it was fair to hypothesize that TiO_2 attaches to MMP3 in the same way that $PtCl_2$ does, potentially inhibiting the enzyme's catalytic activity. Signaling can help to further understand these pathways.

3.6. ADME physicochemical prediction of TiO_2

ADME computational prediction indicated that TiO_2 exhibited a moderate level of absorption in the human intestines (0.81) and a relatively high oral bioavailability (0.84) (Table 2, Fig. 10), making it well above average in terms of absorption capacity. It demonstrated low solubility in water (−6.12 log(mol/L)), suggesting difficulties in dissolving. Its lipophilicity index of 0.97 log-ratio indicated a moderate attraction to lipid environments. The presence of negative hydration-free energy (−2.96 kcal/mol) and low cell permeability (−4.14 log (10-6 cm/s)) indicated substantial obstacles to intracellular penetration. Furthermore, it exhibited a poor permeability of PAMPA (0.33) and little interaction with P-glycoprotein (0.02), indicating restricted efflux activity.

TiO_2 exhibited extensive penetration through the blood-brain barrier (0.99), indicating substantial exposure to the central nervous system. It displayed a high plasma protein binding rate of 87.57%, suggesting significant binding in the circulating blood. The steady-state volume of distribution (0.24 L/kg) indicated restricted dispersion outside the vascular compartment.

With very low percentile values indicating limited interaction potential, TiO_2 exhibited modest inhibition across important cytochrome P450 enzymes, including CYP1A2, CYP2C19, CYP2C9, CYP2D6, and CYP3A4. Furthermore, it demonstrated a low probability of acting as a substrate for CYP2C9 (0.02) and CYP2D6 (0.01), while having somewhat greater potential as a substrate for CYP3A4 (0.25). These characteristics indicated that TiO_2 is improbable to exert a substantial impact on or be affected by metabolic processes that include these enzymes.

TiO_2 exhibited a moderate half-life of 20.26 h, suggesting an extended duration of presence within the human body. Nevertheless, it showed minimal clearance rates in both hepatocytes and microsomes, with values approaching zero, indicating restricted efflux via metabolic pathways. TiO_2 had a significant risk for mutagenicity (0.99) and carcinogenicity (0.85), with percentile levels close to the highest category. Furthermore, it had a notable propensity for drug-induced liver damage (0.88) and a high probability of cutaneous reaction (0.95). The acute toxicity of the compound was rather modest, with an LD_{50} of 1.73 log(1/(mol/kg)). However, its hERG blocking (1.68e-03) and androgen receptor interaction were minimal, indicating poor cardiotoxicity and androgenic activity. Furthermore, it had limited interaction with nuclear factor pathways and mitochondrial membrane potential, suggesting a particular impact on cellular stress responses and energy control (Table 2).

4. Discussion

The biological synthesis of nanoparticles is gaining broad consideration due to the varied areas of applications it offers. Using microbes and plants in nanoparticle synthesis is the most eco-friendly cost-effective approach, which provides economic benefits and a lower damaging environmental effect than conventional chemical synthesis (Loshchinina et al., 2022). Fungi have demonstrated varied capabilities in affecting metal speciation, toxicity, mobility and mineral formation, dissolution or deterioration through diverse biochemical processes. One of these metal interactions is the bioproduction of nanoparticles, which could be in the form of element, mineral or compound. These fungi could benefit from such nano-formation through the removal of metal toxicity or protection from environmental stress (Li et al., 2022). Fungi offer several advantages since they are usually easily cultivated under controlled fermentation conditions and are well known for their excretion of diverse metabolites and enzymes related to nanoparticle formation. Nanoparticles can be formed intracellularly or extracellularly, the

Table 2
ADME physicochemical properties of TiO_2.

Category	Property	Prediction	Drug Bank Percentile
Absorption	Human Intestinal Absorption	0.81	23.03%
	Oral Bioavailability	0.84	58.82%
	Aqueous Solubility	−6.12	4.58%
	Lipophilicity	0.97	41.61%
	Hydration Free Energy	−2.96	95.89%
	Cell Effective Permeability	−4.14	96.82%
	PAMPA Permeability	0.33	26.48%
	P-glycoprotein Inhibition	0.02	32.69%
Distribution	Blood-Brain Barrier Penetration	0.99	92.09%
	Plasma Protein Binding Rate	87.57	68.94%
	Volume of Distribution at Steady State	0.24	38.58%
Metabolism	CYP1A2 Inhibition	5.96e-04	8.45%
	CYP2C19 Inhibition	3.10e-03	6.48%
	CYP2C9 Inhibition	1.47e-04	2.87%
	CYP2D6 Inhibition	2.80e-04	2.87%
	CYP3A4 Inhibition	4.65e-06	3.57%
	CYP2C9 Substrate	0.02	6.44%
	CYP2D6 Substrate	0.01	2.75%
	CYP3A4 Substrate	0.25	28.31%
Excretion	Half-Life	20.26	67.39%
	Drug Clearance (Hepatocyte)	0.00	2.60%
	Drug Clearance (Microsome)	0.00	12.68%
Toxicity	hERG Blocking	1.68e-03	1.78%
	Clinical Toxicity	0.01	8.34%
	Mutagenicity	0.99	99.50%
	Drug-Induced Liver Injury	0.88	78.56%
	Carcinogenicity	0.85	99.11%
	Acute Toxicity LD50	1.73	11.21%
	Skin Reaction	0.95	97.17%
	Androgen Receptor (Full Length)	2.79e-04	1.16%
	Androgen Receptor	9.70e-04	10.31%
	Aryl Hydrocarbon Receptor	2.75e-04	3.45%
	Aromatase	2.90e-04	8.49%
	Estrogen Receptor (Full Length)	0.04	18.11%
	Estrogen Receptor	1.07e-03	6.82%
	Peroxisome Proliferator-Activated Receptor Gamma	1.84e-04	11.90%
	Nuclear Factor (Erythroid-Derived 2)-Like 2/ARE	0.11	46.22%
	ATPase Family AAA Domain-Containing Protein 5	1.23e-04	7.56%
	Heat Shock Factor Response Element	3.99e-03	26.37%
	Mitochondrial Membrane Potential	1.25e-03	14.42%
	Tumor Protein p53	0.04	62.78%

latter being favorable for easy harvest. Although a lot of literature recently described the use of fungi in the green synthesis of metal nanoparticles, only one article has highlighted the biosynthesis of TiO_2 NPs with the extract of *Trichoderma citrinoviridae,* which demonstrated moderate antibacterial activity against the drug-resistant *Pseudomonas aeruginosa* clinical isolates (Arya, Sonawane, Math et al., 2021; Punitha et al., 2020; Ramya et al., 2022; Vembu et al., 2022; Nilavukkarasi et al., 2022).

This current study contributed to our knowledge of the bio-synthesized TiO_2 NPs' potential as anticancer agents by offering insight into their possible cytotoxic effects on human breast cancer cells. Matrix metalloproteinase-3 (MMP3) is a vital member of the matrix metalloproteinase family involved in different pathophysiological aspects of breast cancer. MMP3 is known for its ability to destroy extracellular matrix components, which modifies the tumor microenvironment and aids in the development of cancer (Mendes et al., 2005; Suhaimi et al., 2020). The role of MMP3 in breast cancer is well-established. It breaks down the physical barriers preventing cancer cells from migrating, changing the behavior of stromal cells surrounding malignant cells. MMP3 affects cell adhesion through extracellular matrix modification, which stimulates malignant features such as increased invasiveness and decreased apoptosis. Furthermore, MMP3 controls the cytokines and growth factors in the tumor microenvironment, enhancing tumor growth and metastasis (Padala et al., 2017; Vergara et al., 2018). Recent research has shown how MMP3 influences chemotherapy efficiency and modulates the immune response. Increased MMP3 levels have been associated with a worse prognosis for patients with breast cancer (Balkhi et al., 2020; Hassan et al., 2015; Lei et al., 2002).

Considering MMP3's crucial role in breast cancer development (Fig. 11), it is considered a suitable target for treatment intervention. MMP3 inhibition may interfere with the mechanisms necessary for tumor growth and metastasis. However, due to its involvement in different physiological activities, it is difficult to obtain particular MMP3 inhibitors due to the possibility of serious side effects (Lei et al., 2002; Phromnoi et al., 2009). Research on selective MMP3 inhibitors and methods to adjust their action is still ongoing. Among these initiatives are the creation of monoclonal antibodies, gene therapy, and small chemical inhibitors. According to Radisky et al. (2017), targeting MMP3 could improve the effectiveness of current treatments by increasing the tumor receptiveness to therapeutic interventions and preventing tumor growth and metastasis.

5. Conclusion

Our study has shed light on the selective cytotoxic effect of the green-synthesized TiO_2 NPs on MCF7 breast cancer cells compared to HepG-2 liver cancer cells. TiO_2 NPs appear to offer a unique treatment pathway by targeting matrix metalloproteinase-3 (MMP3), which is vital in the evolution of breast cancer. These findings present new avenues for investigating the potential use of TiO_2 NPs as adjunct therapeutics for cancer patients. Such developments may mark a substantial improvement in the available alternatives for cancer treatment. However, these intriguing nanoparticles must undergo rigorous in vitro and in vivo

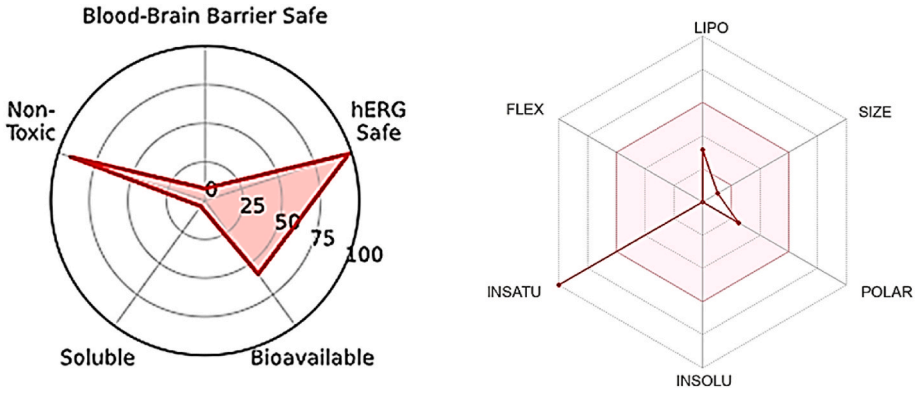

Fig. 10. Bioavailability radar chart of TiO_2.

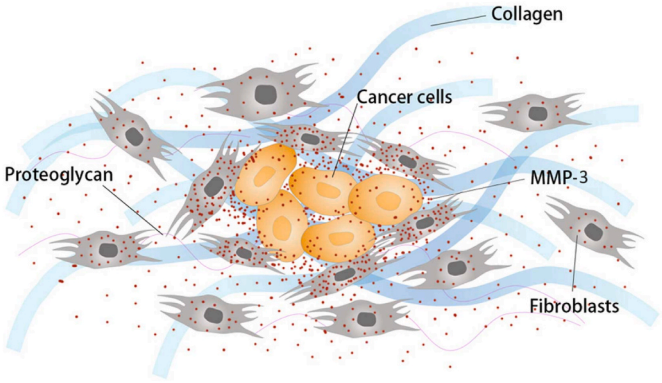

Fig. 11. The pattern of MMP-3 expression within the cancer microenvironment is noteworthy. It is found to be produced by fibroblasts in the cancerous stroma as well as by the cancer cells themselves. Furthermore, MMP-3, a crucial element of the cancer microenvironment, is released into this milieu, impacting the extracellular matrix's (ECM) architecture. This action facilitates the initiation and advancement of tumorigenesis.

studies to fully evaluate their safety and effectiveness.

CRediT authorship contribution statement

Hani A. Alhadrami: Writing – original draft, Validation, Software, Methodology, Investigation, Funding acquisition, Formal analysis. **Hossam M. Hassan:** Writing – original draft, Validation, Project administration, Investigation, Formal analysis, Conceptualization. **Albaraa H. Alhadrami:** Writing – original draft, Software, Resources, Methodology, Formal analysis. **Mostafa E. Rateb:** Writing – review & editing, Supervision, Software, Project administration, Formal analysis, Data curation, Conceptualization. **Ahmed A. Hamed:** Writing – review & editing, Validation, Software, Methodology, Investigation, Formal analysis, Conceptualization.

Informed consent statement

Not applicable.

Institutional review board statement

Not applicable.

Data availability statement

The data generated and presented in this study are available in the manuscript and its supplementary data.

Funding

This work was supported by the Institutional Fund Projects (grant number IFPIP:623-142-1443).

Declaration of competing interest

The authors declare no conflicts of interest.

Acknowledgment

This research work was funded by Institutional Fund Projects under grant no (IFPIP:623-142-1443). The authors gratefully acknowledge the technical and financial support from the Ministry of Education and King Abdulaziz University, DSR, Jeddah, Saudi Arabia.

References

Antić, Ž., Krsmanović, W. R., Nikolic, M., Marinović-Cincović, M., Mitrić, M., Polizzi, S., & Dramicanin, M. (2012). Multisite luminescence of rare earth doped TiO_2 anatase nanoparticles. *Materials Chemistry and Physics, 135*. https://doi.org/10.1016/j.matchemphys.2012.06.016

Armand, L., Belade, E., Duprez, C., Tharabhat, C., Le Gouvello, S., Pairon, J. C., et al. (2011). Effects of titanium dioxide nanoparticles on matrix remodeling markers in human pulmonary fibroblasts. In *Nanoparticles, A2280-A2280*. American Thoracic Society.

Arya, S., Sonawane, H., Math, S., et al. (2021). Biogenic titanium nanoparticles (TiO_2NPs) from *Tricoderma citrinoviride* extract: Synthesis, characterization and antibacterial activity against extremely drug-resistant Pseudomonas aeruginosa. *International Nano Letters, 11*, 35–42. https://doi.org/10.1007/s40089-020-00320-y

Ba-Abbad, M., Kadhum, A. H., Mohamad, A., Takriff, M. S., & Sopian, K. (2019). Synthesis and catalytic activity of TiO_2 nanoparticles for photochemical oxidation of concentrated chlorophenols under direct solar radiation. *Microorganisms, 7*(12), 102.

Balkhi, S., Mashayekhi, F., Salehzadeh, A., & Saedi, H. S. (2020). Matrix metalloproteinase (MMP)-1 and MMP-3 gene variations affect MMP-1 and -3 serum concentration and associate with breast cancer. *Molecular Biology Reports, 47*(12), 9637–9644.

Belviso, B. D., Caliandro, R., Siliqi, D., Calderone, V., Arnesano, F., & Natile, G. (2013). Structure of matrix metalloproteinase-3 with a platinum-based inhibitor. *Chemical Communications, 49*(48), 5492–5494.

Dzulkharnien, N. S. F., & Rohani, R. (2022). A review on current designation of metallic nanocomposite hydrogel in biomedical applications. *Nanomaterials, 12*(9), 1629.

Elkhouly, H. I., Hamed, A. A., Hosainy, A. M., Ghareeb, M. A., & Sidkey, N. M. (2021). Bioactive secondary metabolite from endophytic Aspergillus tubenginses ASH4 isolated from Hyoscyamus muticus: Antimicrobial, antibiofilm, antioxidant, and anticancer activity. *Microorganisms, 11*(2), 102.

Hassan, S. A., Hammam, O., Htwe, T. T., & Ghanem, H. Z. (2015). Possible diagnostic/prognostic role of survivin and MMP3 in breast cancer disease. *Journal of Multidisciplinary Engineering Science and Technology, 2*, 3121–3127.

Humphrey, W., Dalke, A., & Schulten, K. (1996). Vmd: Visual molecular dynamics. *Microorganisms, 7*(1), 38.

Khan, S. T., & Sultana, T. (2019). Applications of titanium dioxide nanoparticles in wastewater treatment: A review. *Microorganisms, 7*(12), 689.

Komine, C., Uchibori, S., Tsudukibashi, O., & Tsujimoto, Y. (2022). Application of reactive oxygen species in dental treatment. *Microorganisms, 12*(9), 1531.

Kumar, S., Stecher, G., Li, M., Knyaz, C., & Tamura, K. (2018). Mega X: Molecular evolutionary genetics analysis across computing platforms. *Microorganisms, 6*(10), 102.

Lei, H., Zaloudik, J., & Vorechovsky, I. (2002). Lack of association of the−1171 (5A) allele of the MMP3 promoter with breast cancer. *Clinical Chemistry, 48*(5), 798–799.

Li, L., Chen, D., Zhang, Y., & Wei, Q. (2019). A review on the visible light active titanium dioxide photocatalysts for environmental applications. *Microorganisms, 7*(6), 167.

Li, Q., Liu, F., Li, M., Chen, C., & Gadd, G. M. (2022). Nanoparticle and nanomineral production by fungi. *Fungal Biol. Reviews, 41*, 31–44. https://doi.org/10.1016/j.fbr.2021.07.003

Loshchinina, E. A., Vetchinkina, E. P., & Kupryashina, M. A. (2022). Diversity of biogenic nanoparticles obtained by the fungi-mediated synthesis: A review. *Biomimetics, 8*(1). https://doi.org/10.3390/biomimetics8010001

Mendes, O., Kim, H. T., & Stoica, G. (2005). Expression of MMP2, MMP9, and MMP3 in breast cancer brain metastasis in a rat model. *Clinical & Experimental Metastasis, 22*, 237–246.

Miller III, B. R., McGee Jr, T. D., Swails, J. M., Homeyer, N., Gohlke, H., & Roitberg, A. E. (2012). MMPBSA.py: An efficient program for end-state free energy calculations. *Microorganisms, 8*(11), 102.

Nasr, R., Hasanzadeh, H., Khaleghian, A., Moshtaghian, A., Emadi, A., & Moshfegh, S. (2018). Induction of apoptosis and inhibition of invasion in gastric cancer cells by titanium dioxide nanoparticles. *Microorganisms, 7*(2), 102.

Nilavukkarasi, M., Vijayakumar, S., Kalaskar, M., Gurav, N., Gurav, S., & Praseetha, P. K. (2022). Capparis zeylanica L. conjugated TiO2 nanoparticles as bio-enhancers for antimicrobial and chronic wound repair. *Biochemical and Biophysical Research Communications, 623*, 127–132. https://doi.org/10.1016/j.bbrc.2022.07.064

Padala, C., Tupurani, M. A., Puranam, K., Gantala, S., Shyamala, N., … Hanumanth, S. R. (2017). Synergistic effect of collagenase-1 (MMP1), stromelysin-1 (MMP3), and gelatinase-B (MMP9) gene polymorphisms in breast cancer. *PLoS One, 12*(9), Article e0184448.

Phan, H. T., & Haes, A. J. (2020). What does nanoparticle stability mean? *Microorganisms, 7*(7), 102.

Phillips, J. C., Braun, R., Wang, W., Gumbart, J., Tajkhorshid, E., Villa, E., Chipot, C., Skeel, R. D., Kalé, L., & Schulten, K. (2005). Scalable molecular dynamics with NAMD. *Microorganisms, 7*(10), 102.

Phromnoi, K., Yodkeeree, S., Anuchapreeda, S., & Limtrakul, P. (2009). Inhibition of MMP-3 activity and invasion of the MDA-MB-231 human invasive breast carcinoma cell line by bioflavonoids. *Acta Pharmacologica Sinica, 30*(8), 1169–1176.

Punitha, V. N., Vijayakumar, S., Sakthivel, B., & Praseetha, P. K. (2020). Protection of neuronal cell lines, antimicrobial and photocatalytic behaviors of eco-friendly TiO2 nanoparticles. *Journal of Environmental Chemical Engineering, 8*, Article 104343. https://doi.org/10.1016/j.jece.2020.104343

Radisky, E. S., Raeeszadeh-Sarmazdeh, M., & Radisky, D. C. (2017). Therapeutic potential of matrix metalloproteinase inhibition in breast cancer. *Journal of Cellular Biochemistry, 118*(11), 3531–3548.

Ramya, S., Vijayakumar, S., Vidhya, E., Bukhari, N. A., Hatamleh, A. A., Nilavukkarasi, M., Vijayakumar, S., & Pham, T. H. (2022). TiO2 nanoparticles

derived from egg shell waste: Eco synthesis, characterization, biological and photocatalytic applications. *Environmental Research, 214*(Pt 1), Article 113829. https://doi.org/10.1016/j.envres.2022.113829

Ribeiro, J. V., Bernardi, R. C., Rudack, T., Schulten, K., & Tajkhorshid, E. (2018). QwikMD-Gateway for easy simulation with VMD and NAMD. *Microorganisms, 11*(3), 102.

Setty, S. (2020). Spartan: Efficient and general-purpose zkSNARKs without trusted setup. *Microorganisms, 8*(9), 102.

Shyamalagowri, S., et al. (2022). In vitro anticancer activity of silver nanoparticles phyto-fabricated by Hylocereus undatus peel extracts on human liver carcinoma (HepG2) cell lines. *Process Biochemistry, 116*, 17–25.

Suhaimi, S. A., Chan, S. C., & Rosli, R. (2020). Matrix metallopeptidase 3 polymorphisms: Emerging genetic markers in human breast cancer metastasis. *Journal of Breast Cancer, 23*, 1–9.

Swanson, K., Walther, P., Leitz, J., Souhrid Mukherjee, S., et al. (2024). ADMET-AI: A machine learning ADMET platform for evaluation of large-scale chemical libraries. *Bioinformatics, 40*, Article btae416. https://doi.org/10.1093/bioinformatics/btae416

Tamura, K., Nei, M., & Kumar, S. (2004). Prospects for inferring very large phylogenies by using the neighbor-joining method. *Microorganisms, 7*(9), 102.

Thamaphat, K., Limsuwan, P., & Ngotawornchai, B. (2019). Phase characterization of TiO2 powder by XRD and TEM. *Microorganisms, 6*(3), 102.

Varshney, R., Bhadauria, S., & Gaur, M. S. (2019). Biogenic synthesis of silver nanocubes and nanorods using sundried Stevia rebaudiana leaves. *Microorganisms, 1*(3), 237.

Vembu, S., Vijayakumar, S., Nilavukkarasi, M., Vidhya, E., & Punitha, V. N. (2022). Phytosynthesis of TiO2 nanoparticles in diverse applications: What is the exact mechanism of action? *Sensors International, 3*, Article 100161. https://doi.org/10.1016/j.sintl.2022.100161

Vergara, M. C. M., Hartland, E., Jang, C., McGarel, M., Moreno, R. R., Kaliney, W., … Littlepage, L. E. (2018). Stromal MMP3 inhibits oncogenic potential during breast cancer progression. *Cancer Research, 78*(13_Supplement), 5078, 5078.

Waghmode, M. S., Gunjal, A. B., Mulla, J. A., et al. (2019). Studies on the titanium dioxide nanoparticles: Biosynthesis, applications, and remediation. *SN Applied Sciences, 1*, 310. https://doi.org/10.1007/s42452-019-0337-3

Ziental, D., Czarczynska-Goslinska, B., Mlynarczyk, D. T., Glowacka-Sobotta, A., Stanisz, B., Goslinski, T., & Sobotta, L. (2020). Titanium dioxide nanoparticles: Prospects and applications in medicine. *Nanomaterials, 10*(2), 387. https://doi.org/10.3390/nano10020387